

Received 22 September 2022; accepted 26 October 2022. Date of publication 31 October 2022; date of current version 7 November 2022.  
 The review of this article was arranged by Editor Munaf T. A. Rahimo.

Digital Object Identifier 10.1109/JEDS.2022.3218020

# Experimental Investigation and Model Analysis on a GaN Electrostatic Discharge Clamp

YIJUN SHI<sup>ID</sup><sup>1</sup>, ZHIYUAN HE<sup>ID</sup><sup>1</sup>, YUN HUANG<sup>1</sup> (Member, IEEE), ZONGQI CAI<sup>ID</sup><sup>1</sup>,  
 YIQIANG CHEN<sup>ID</sup><sup>1</sup> (Member, IEEE), CHANG LIU<sup>ID</sup><sup>1</sup>, CHAO LIU<sup>ID</sup><sup>2</sup>, WANJUN CHEN<sup>ID</sup><sup>2</sup> (Senior Member, IEEE),  
 RUIZE SUN<sup>ID</sup><sup>2</sup> (Member, IEEE), AND GUOGUANG LU<sup>1</sup>

<sup>1</sup> China Electronic Product Reliability and Environmental Testing Research Institute, Guangzhou 510610, China

<sup>2</sup> State Key Laboratory of Electronic Thin Films and Integrated Devices, University of Electronic Science and Technology of China, Chengdu 610054, China

CORRESPONDING AUTHORS: Z. HE, Y. CHEN, and C. LIU (e-mail: hezhiyuan1988@126.com; yiqiang-chen@hotmail.com; chaoliu@uestc.edu.cn)

This work was supported in part by the National Natural Science Foundation of China (NSFC) under Grant 62004046; in part by the Key-Area Research and Development Program of Guangdong Province under Grant 2020B010173001; and in part by the Natural Science Foundation of Guangdong Province under Grant 2022A1515012127.

**ABSTRACT** This work carried out the experimental investigation and model analysis on a GaN electrostatic discharge (ESD) clamp, which features a discharge high electron mobility transistor (HEMT) and a voltage divider formed by a lateral field effect rectifier (L-FER) chain and a resistor in series. Firstly, it is found through the experimental investigation, the turn-on voltage ( $V_T$ ) of GaN ESD clamp's static current is increased with the increase in L-FER's number and the decrease in resistor's value. Then, an analytical model is proposed to analyze the dependence of  $V_T$  on L-FER's number and resistor's value. And the analytical model exhibits a good consistency with the experimentally measured results, which confirms the validity of the presented analytical model. Lastly, the dependence of GaN ESD clamp's transmission line pulsing characteristics on the L-FER's number and resistor's value is also analyzed. Similarly, GaN ESD clamp's triggering voltage is also increased with the increase in L-FER's number and the decrease in resistor's value. The experimental investigation and model analysis of this work can be used to direct the design of GaN ESD clamp, and help to save a lot of manpower, material resources and time costs.

**INDEX TERMS** Electrostatic discharge, ESD clamp, GaN HEMT, triggering voltage, human body model.

## I. INTRODUCTION

In the field of power electronics, the degradation or failure induced by electrostatic discharge (ESD) event has attracted more and more attention [1], [2], [3], [4], [5], [6], [7]. It is because, the ESD-induced instantaneous high voltage will damage electronic components' sensitive structures and their internal connections, which accounts for more than 60% of the events causing the failure of electronic components. Especially for the power electronic devices with insulated gate and semi-insulated gate, namely p-GaN high electron mobility transistors (HEMTs), there is no effective channel in their gate structure to discharge the electrostatic charges, which makes their gate structure easily be damaged by ESD event [7], [8], [9], [10], [11]. It has been demonstrated that the gate structure of p-GaN HEMT exhibits poor ESD robustness, with an equivalent human body model (HBM) failure

voltage ( $V_{HBM}$ ) of only 0.2~0.33 kV, which is far below the industrial standard (2 kV) [11].

Effectively improving the gate structure's ESD reliability of p-GaN HEMTs has always been the focus of attention. And different from the vertical power electronic devices, it is relatively convenient to monolithically integrate the ESD protection structures and other protecting circuits into GaN-based lateral power electronic devices [12], [13], [14], [15]. In this way, the parasitic parameters of power electronic systems can be decreased to a certain extent, which will improve the performance of power electronic systems. So, there are some efforts to design the effective GaN lateral ESD protection structures, which are able to be monolithically integrated into GaN lateral power devices to improve devices' ESD reliability. Wang et al. have presented a GaN lateral ESD protection structure featuring a discharge HEMT,

a turn-off diode chain, and a voltage divider formed by a trigger diode chain and a current limiting resistor [16]. The ESD protection structure is capable of discharging the forward transient current up to 3A, but it can do nothing to discharge the transient accumulated charge in reverse ESD events. So, that ESD protection structure may be not suitable to effectively protect the gate structure of p-GaN HEMT. To usefully enhance p-GaN HEMT's ESD reliability in both the forward and reverse ESD events, Zhou et al. have presented a novel GaN lateral ESD protection structures [17], which features a discharge HEMT and a voltage divider formed by two lateral field effect rectifiers (L-FERs) and a resistor in series. The ESD protection structure can discharge forward transient charge and reverse transient charge at the same time. But the influence of L-FER's number and resistor's value on the ESD protection structure's characteristic is not clearly. And there is no relevant analysis model to direct the design of GaN ESD protection structure. For obtaining a desirable ESD protection structure, the design engineers need to experiment repeatedly, which will cost a lot of manpower, material resources and time costs.

In this work, we carried out the experimental investigation and model analysis on a GaN ESD clamp, which features a discharge HEMT and a voltage divider formed by a L-FER chain and a resistor in series. It is found that the L-FER's number and resistor's value play an important role on the characteristic of GaN ESD clamp. And we proposed an analytical model to analyze the dependence of clamp's static turn-on voltage ( $V_T$ , defined as the point where the static current suddenly is increased) on the L-FER's number and resistor's value. Then, the dependence of ESD clamp's transmission line pulsing (TLP) characteristic on the L-FER's number and resistor's value is also analyzed. The manuscript is organized as follows: The structure and mechanism of the studied GaN ESD clamp are briefly introduced in Section II; The influence of L-FER's number and resistor's value on the ESD clamp's static characteristic are investigated and modeled in Section III; The ESD clamp's transmission line pulsing (TLP) characteristics are analyzed in Section IV; The conclusion is given in Section V.

## II. STRUCTURE AND MECHANISM

Before introducing GaN ESD clamp in [17], it may be necessary to briefly introduce the influence of the voltage overshoots on the reliability of conventional p-GaN HEMT. Fig. 1 gives the bidirectional TLP characteristics of P-GaN HEMT and its gate-to-source leakage current ( $I_{GSS}$ ) before/after the forward/reverse ESD breakdown (FB/RB). The device's forward and reverse ESD breakdown are occurred at 261V and 300V, respectively. After that, the device's  $I_{GSS}$  exhibits a significant increase. Therefore, it is necessary to improve the gate structure's ESD reliability for the existing E-mode p-GaN HEMTs. In this work, we carried out the experimental investigation and model analysis on a GaN ESD clamp, which can be used to direct the ESD design of the existing E-mode p-GaN HEMTs.

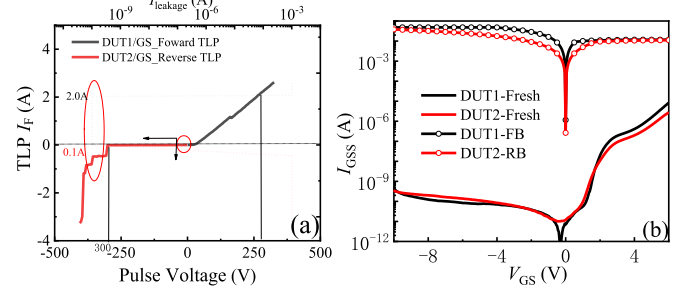


**FIGURE 1.** (a) The bidirectional TLP characteristics of p-GaN HEMT (GS-065-011-1-L), (b) p-GaN HEMT's  $I_{GSS}$  before and after the forward/reverse ESD breakdown.

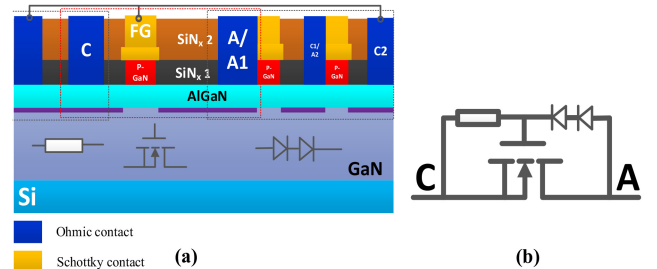


**FIGURE 2.** (a) The structure and (b) equivalent circuit of the GaN ESD clamp featuring a discharge HEMT and a voltage divide.

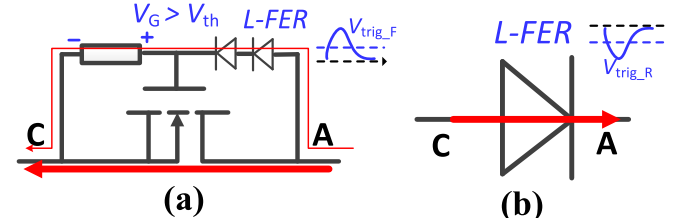


**FIGURE 3.** The mechanism of GaN ESD clamp featuring a discharge HEMT and a voltage divider: (a) in forward ESD event, (b) in reverse ESD event.

Fig. 2 shows the structure and equivalent circuit of GaN ESD clamp in [17]. The clamp features a GaN discharge HEMT and a voltage divider formed by a L-FER chain and a resistor in series. And the mechanism of GaN ESD clamp is shown in Fig. 3. In the forward ESD event or with a forward static voltage applied at the anode electrode, there will be a small current flowing through the L-FER chain and resistor, which will result in a voltage drop between GaN discharge HEMT's gate and cathode. When the voltage drop is higher than the threshold voltage ( $V_{th}$ ) of GaN discharge HEMT, which will be turned on. Afterwards, the forward electrostatic charges induced by ESD event can be released through the GaN discharge HEMT (Fig. 3 (a)), or the large static current can flow through the GaN discharge HEMT. Thereby, the potential of the clamp's anode electrode can be clamped to a small value. And the degradation or failure induced by the ESD event can be avoided. It can be surmised, the L-FER's number and resistor's value act as significant roles on the forward triggering voltage ( $V_{trig\_F}$ ,

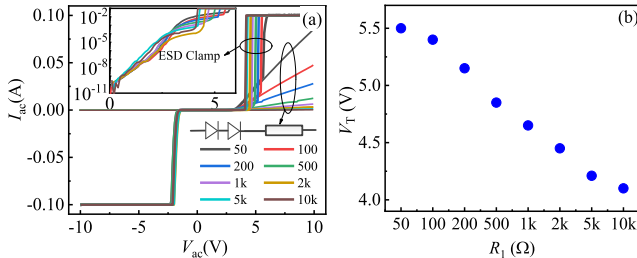


**FIGURE 4.** The influence of resistor's value on the GaN ESD clamp's static current characteristic (a) and forward turn-on voltage (b). There are two L-FERs in the voltage divider.

defined at a forward TLP current density of 0.1A for this work) and forward  $V_T$  ( $V_{T\_F}$ , defined as the point where the forward static current suddenly increases) of GaN ESD clamp. The increase in L-FER's number and the decrease in resistor's value can lead to the increase in  $V_{trig\_F}$  and  $V_{T\_F}$ . So, through changing the L-FER's number or resistor's value, a desirable  $V_{trig\_F}$  and  $V_{T\_F}$  can also be obtained. In the reverse ESD event or with a reverse static voltage applied at the anode electrode, the GaN ESD clamp conduct current in diode mode (Fig. 3 (b)) and has a low reverse triggering voltage ( $V_{trig\_R}$ , defined at a reverse TLP current density of 0.1A for this work) or low reverse  $V_T$  ( $V_{T\_R}$ , defined as the point where the reverse static current suddenly increases). The changes in the L-FER's number or resistor's value nearly have no effect on the clamp's  $V_{trig\_R}$  and  $V_{T\_R}$ .

The specific influence of the L-FER's number and resistor's value on GaN ESD clamp's characteristic is still not clearly. And there is no relevant analysis model to direct the design of GaN ESD clamp. For obtaining a desirable GaN ESD clamp, the design engineers need to experiment repeatedly, which will cost a lot of manpower and material resources. Based on the above reasons, we carried out the experimental investigation and model analysis on the GaN ESD clamp. Similar to our previous work [18], [19], for reducing the experimental cost, the equivalent structure made up of the chip resistor and p-GaN HEMTs (EPC2036) [20] is employed to carry out the experimental investigation. As noted, due to the lack of commercial GaN L-FER, L-FER in GaN ESD clamp is also made up of commercial p-GaN HEMT (EPC2036). Corresponding device information can be found in [20]. The short connection of the source and gate electrode of p-GaN HEMT is regarded as the L-FER's anode electrode, and the drain electrode of p-GaN HEMT is regarded as the L-FER's cathode electrode. Our self-developed TLP measurement system is employed to produce TLP pulses. The rising time ( $t_r$ ) and pulse width ( $t_w$ ) in TLP tests are set to be 2 and 100 ns, respectively [18], [19].

### III. STATIC CHARACTERISTIC AND MODEL

Fig. 4 gives the dependence of GaN ESD clamp's static current characteristics on the resistor's value of voltage divider.

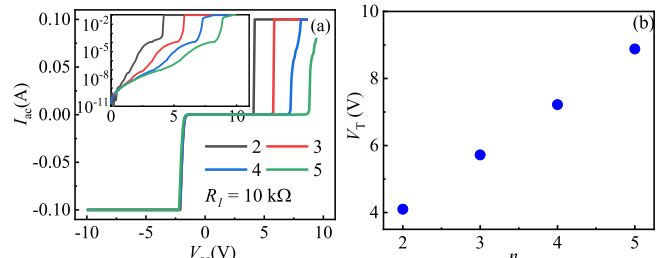


**FIGURE 5.** The influence of L-FER's number on the GaN ESD clamp's static current characteristic (a) and forward turn-on voltage (b). The resistor's value is  $10\text{ k}\Omega$ .

It can be found, the forward turn-on voltage of GaN ESD clamp's static current is decreased with the increase in resistor's value. When the resistor's value is increased from  $50\text{ }\Omega$  to  $10\text{ k}\Omega$ , the GaN ESD clamp's forward turn-on voltage is decreased from  $5.5\text{ V}$  to  $4.1\text{ V}$  (as summarized in Fig. 4 (b)). However, although the GaN ESD clamp with a small resistor can possess a relatively high forward turn-on voltage, the small resistor in the voltage divider will lead to a high static leakage current before the GaN discharge HEMT are turned on (as also shown in Fig. 4 (a)), which is not desired in the field of power electronics. So, to avoid this phenomenon, a relatively large resistor (over than  $1\text{ k}\Omega$  in this work) or a small-size L-FER in the voltage divider is preferable. Meanwhile, as stated above, with a reverse static voltage applied at the anode electrode, the GaN ESD clamp conduct current in diode mode, and has a low reverse turn-on voltage. The changes in the resistor's value nearly have no effect on the GaN ESD clamp's reverse turn-on voltage (as shown in Fig. 4 (a)).

Compared with regulating the clamp's forward turn-on voltage by changing the resistor's value of the voltage divider, changing the L-FER's number has a more obvious effect, the reasons for this phenomenon can be interpreted by our analytical model in following. Fig. 5 (a) gives the influence of the L-FER's number on the GaN ESD clamp's static current. The forward turn-on voltage of GaN ESD clamp's static current is increased with the increase in L-FER's number. When the L-FER's number is increased from 2 to 5, the clamp's forward turn-on voltage is increased from  $4.1\text{ V}$  to  $8.9\text{ V}$  (as summarized in Fig. 5 (b)). So, through changing the L-FER's number and the resistor's value, a desirable forward turn-on voltage can be obtained for the GaN ESD clamp. Similarly, the changes in the L-FER's number nearly have no effect on the GaN ESD clamp's reverse turn-on voltage (Fig. 5 (a)).

In order to give more clear guidance to designers, an analytical model is proposed to analyze the dependence of the clamp's forward turn-on voltage on the L-FER's number and resistor's value. At first, the gate voltage ( $V_G$ ) of GaN discharge HEMT is equal to the voltage drop at the resistor and can be calculated through eq. (1).

$$V_G = I_{F1} \times R_1 \quad (1)$$

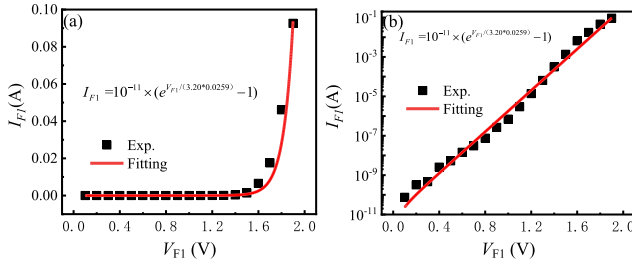


**FIGURE 6.** The L-FER's forward current fitted by eq. (3) (solid line), and the experimentally measured results (dots).

where  $I_{F1}$  is the current flowing through the resistor,  $R_1$  is the resistor's value. As stated above, when the gate voltage is equal to the threshold voltage of the GaN discharge HEMT, which will be turned on. Afterwards, the large static current can flow through the GaN discharge HEMT. In this time, the current flowing through the resistor can be estimated through eq. (2).

$$I_{F1} = \frac{V_G}{R_1} = \frac{V_{th}}{R_1} \quad (2)$$

From eq. (1), it can be found that the current flowing through the resistor is prerequisite to calculate the gate voltage of GaN discharge HEMT. And the current flowing through the resistor is same as that in each L-FER, which can be calculated through eq. (3) [21], [22].

$$I_{F1} = I_{FO} \times \left( e^{q(V_{F1} - I_{FO} \cdot R_s)/nkT} - 1 \right) \quad (3)$$

where  $V_{F1}$  is the voltage drops at each L-FER,  $I_{FO}$  is the saturation current,  $R_s$  is the device linear resistance,  $n$  is the ideal factor of L-FER,  $k$  is Boltzmann constant,  $T$  is thermodynamic temperature. For fitting the experimentally measured forward current characteristics of EPC2036 with eq. (3),  $I_{FO} \times R_s$  is ignored (due to that the linear resistance of L-FER is relatively small),  $I_{FO}$  and  $n$  are equal to  $10^{-11}\text{ A}$  and 3.20, respectively. Fig. 6 gives the L-FER's forward current fitted by eq. (4) and the experimentally measured forward current characteristics. There is no obvious difference between the fitting results and experimentally measured results, which demonstrates the correctness and accuracy of eq. (4).

$$\begin{aligned} I_{F1} &= I_{FO} \times \left( e^{qV_{F1}/nkT} - 1 \right) \\ &= 10^{-11} \times \left( e^{V_{F1}/3.2*0.0259} - 1 \right) \end{aligned} \quad (4)$$

Then, eq. (3) can be transformed to eq. (5), and the voltage drops at each L-FER ( $V_{F1}$ ) can be obtained.

$$V_{F1} = nkT \ln \left( \frac{I_{F1}}{I_{FO}} + 1 \right) / q \quad (5)$$

The voltage needed to turn on the GaN ESD clamp ( $V_T$ ) is the sum of the voltage drops at L-FER chain and the

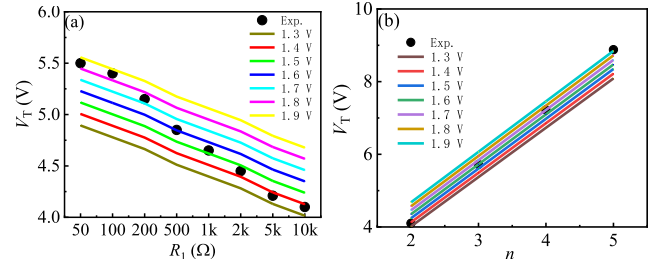


**FIGURE 7.** The influence of the resistor's value (a) and L-FER's number (b) on the ESD clamp's forward turn-on voltage from the presented analytical model and experimentally measured results.

voltage drop at the resistor, as shown in eq. (6).

$$\begin{aligned} V_F &= I_{F1}R_1 + mV_{F1} \\ &= V_G + mnkT \ln \left( \frac{I_{F1}}{I_{FO}} + 1 \right) / q \end{aligned} \quad (6)$$

where  $m$  is the L-FER's number, the first term ( $I_{F1} \times R_1$ ) in eq. (6) is the voltage drop at the resistor or the gate voltage ( $V_G$ ) of GaN discharge HEMT, the second term ( $mV_{F1}$ ) is the voltage drops at L-FER chain. It is assumed in eq. (6) that the voltage drops at every L-FER is coincident. Through combining eq. (2) and eq. (6), the ESD clamp's forward turn-on voltage can be obtained, as shown in eq. (7):

$$\begin{aligned} V_T &= V_F = V_G + mV_{F1} \\ &= I_{F1}R_1 + mnkT \ln \left( \frac{I_{F1}}{I_{FO}} + 1 \right) / q \\ &= V_{th} + mnkT \ln \left( \frac{V_{th}/R_1}{I_{FO}} + 1 \right) / q \end{aligned} \quad (7)$$

When  $V_{th}$  adopted in the presented analytical model (eq. (7)) is explicit, the dependence of the ESD clamp's forward turn-on voltage on the L-FER's number and resistor's value can be obtained. It can be speculated from the presented analytical model, the forward turn-on voltage of the GaN ESD clamp's static current is increased with the increase in L-FER's number ( $m$ ) and the decrease in resistor's value ( $R_1$ ), which is consistent with the experimentally measured results. And compared with regulating the ESD clamp's forward turn-on voltage by changing the resistor's value in the voltage divider, changing the L-FER's number has a more obvious effect. Fig. 6 exhibits the influence of the L-FER's number and resistor's value on the ESD clamp's forward turn-on voltage from the presented analytical model with different adopted  $V_{th}$ , accompanied with the experimentally measured results. It can be seen that, when the adopted  $V_{th}$  in the presented analytical model is equal to the threshold voltage (1.6 V) of the GaN discharge HEMT, the ESD clamp's forward turn-on voltage from the presented analytical model exhibits a good agreement with the experimentally measured results, as shown in Fig. 7. In this case, the maximum error between the clamp's forward turn-on voltages from the presented analytical model and the experimentally measured results is 0.27V, and the corresponding mean

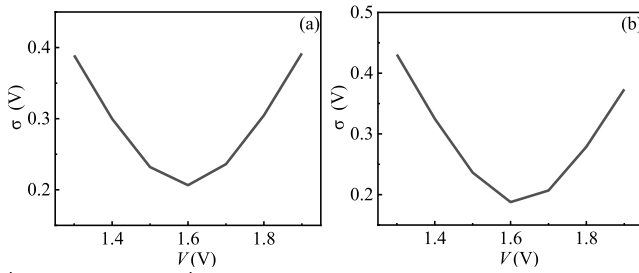


**FIGURE 8.** The error analysis of the ESD clamp's forward turn-on voltage from the presented analytical model and the experimentally measured results: (a) corresponding to Fig. 6 (a), (b) corresponding to Fig. 6 (b).

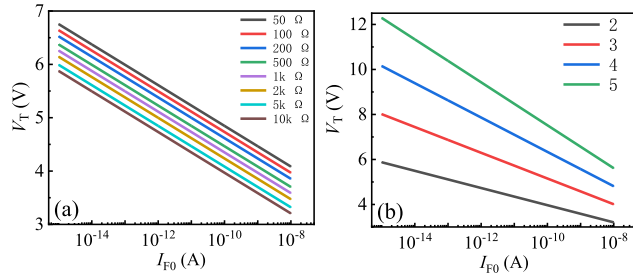


**FIGURE 9.** The influence of  $I_{F0}$  on the forward turn-on voltage of the ESD clamp with different resistor's value (a) and different L-FER's number (b).

square deviation ( $\sigma$ ) is 0.18 V. In addition, when the adopted  $V_{th}$  in the presented analytical model is different from the threshold voltage of the GaN discharge HEMT, the clamp's forward turn-on voltage from the presented analytical model will exhibit inferior agreement with the experimentally measured results. Namely, when the adopted  $V_{th}$  in the presented analytical model is 1.3 V, the maximum error between the clamp's forward turn-on voltages from the presented analytical model and the experimentally measured results is about 0.8 V (as shown in Fig. 7 (b)), and the corresponding mean square deviation is about 0.4V (as shown in Fig. 8 (b)). Therefore, in order to accurately predict the static turn-on voltage of GaN ESD clamp, the accurate threshold voltage of the GaN discharge HEMT is needed. Even with a small error in the threshold voltage of GaN discharge HEMT, it will produce a poor agreement with the experimentally measured results.

Besides the resistor's value and L-FER's number, the ESD clamp's forward turn-on voltage is also dependent on the L-FER's size, which can be quantified by the L-FER's saturation current ( $I_{F0}$ ). And the L-FER's saturation current is increased with the increase in L-FER's size. Fig. 9 gives the dependence of the ESD clamp's forward turn-on voltage on the L-FER's saturation current, which is calculated from the presented analytical model. It can be found, the forward turn-on voltage of the GaN ESD clamp's static current is decreased with the increase in L-FER's saturation current. For the ESD clamp with a  $10k\Omega$  resistor and two L-FERs, its forward turn-on voltage is decreased from 5.87V to 3.21V with the L-FER's saturation current increased from

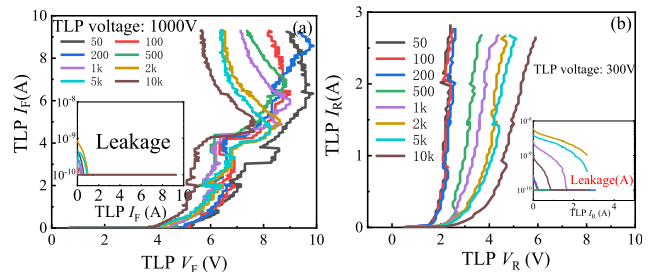


**FIGURE 10.** The influence of the resistor's value on the GaN ESD clamp's forward TLP characteristics (a) and reverse TLP characteristics (b). There are two L-FERs in the voltage divider.

$10^{-15}$  A to  $10^{-8}$  A. It is because that, when the L-FER possesses a higher saturation current, the voltage drop on the voltage divider's resistor will be increased. So, to obtain a preferable forward turn-on voltage for the GaN ESD clamp, changing the L-FER's size may be also a good choice. By comparison, the L-FER with low saturation current is more preferable, due to that it will lead to a low leakage for the GaN ESD clamp and can avoid premature turn-on of the static current, which is serious for the L-FER with high saturation current, as shown in Fig. 4(a). And it can also be found in Fig. 9 (b), the change in the L-FER's saturation current has a more obvious effect on the forward turn-on voltage of the ESD clamp with more L-FERs. For the ESD clamp with a  $10k\Omega$  resistor and five L-FERs, its forward turn-on voltage is decreased from 12.29V to 5.61V with the L-FER's saturation current increased from  $10^{-15}$  A to  $10^{-8}$  A. The change amount is 6.68V, which is higher than that of the ESD clamp with two L-FERs.

#### IV. TLP CHARACTERISTIC

Fig. 10 gives the dependence of the GaN ESD clamp's TLP  $I-V$  characteristics on the resistor's value of the voltage divider. In the positive TLP test, the GaN ESD clamp can be triggered at a low voltage of less than 6 V and possesses a high second breakdown current ( $I_S$ , the current at the forward/reverse ESD breakdown) of over than 9 A, showing that the GaN ESD clamp can effectively discharge the transient electrostatic charges and clamp the potential at a low value, thereby effectively protecting the gate structure of p-GaN HEMT. It also can be found, the forward triggering voltage of GaN ESD clamp is decreased with the increase in resistor's value. When the resistor's value is increased from  $50\Omega$  to  $10k\Omega$ , the GaN ESD clamp's forward triggering voltage is decreased from 5.3 V to 3.9 V (Fig. 12 (a)). So, through changing the resistor's value, a desirable forward triggering voltage can be obtained for the GaN ESD clamp. However, it should be noted that the GaN ESD clamp with a low triggering voltage will possess a low turn-on voltage of the static current. The designers should try to avoid premature turn-on of the static current before obtaining a low triggering voltage in the transient ESD event. In addition, all the GaN ESD clamps possess a high second breakdown current of over than 9 A. Correspondingly, the equivalent HBM failure voltage

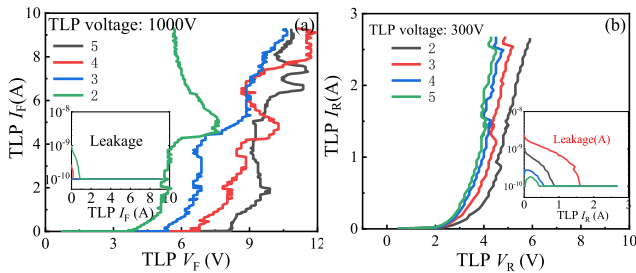


**FIGURE 11.** The influence of L-FER's number on the GaN ESD clamp's forward TLP characteristics (a) and reverse TLP characteristics (b). The resistor's value is  $10\text{ k}\Omega$ .

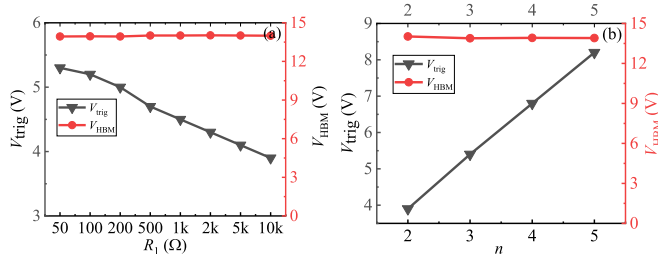


**FIGURE 12.** Forward  $V_{\text{trig}}$  and  $V_{\text{HBM}}$  of the GaN ESD clamp with different resistor's value (a) and different L-FER's number (b).

( $V_{\text{HBM}} = I_S \times 1500\text{ }\Omega$ ) reaches to 13.5 kV (Fig. 12 (a)). In the reverse ESD event, the reverse triggering voltage of the GaN ESD clamp is increased with the increase in the resistor's value (Fig. 10 (b)), which is different from the clamp's forward TLP characteristics and may result from the RC delay caused by the resistor between the cathode/source and the gate of GaN discharge HEMT. When the resistor's value is increased from  $50\text{ }\Omega$  to  $10\text{ k}\Omega$ , the GaN ESD clamp's forward triggering voltage is increased from 1.8 V to 2.4 V. Although the changes in the resistor's value have definite effect on the GaN ESD clamp's reverse triggering voltage, the value is much smaller than the working voltage of p-GaN HEMT.

Compared with regulating the clamp's forward triggering voltage by changing resistor's value in the voltage divider, changing L-FER's number has a more obvious effect. Fig. 11 gives the influence of L-FER's number on the GaN ESD clamp's TLP characteristics. The forward triggering voltage of the GaN ESD clamp is increased with the increase in L-FER's number. When the L-FER's number is increased from 2 to 5, the clamp's forward triggering voltage is increased from 3.9 V to 8.2 V (Fig. 12 (b)). So, through changing the L-FER's number, a desirable forward triggering voltage can be obtained for the GaN ESD clamp. In addition, all the GaN ESD clamps possess a high  $V_{\text{HBM}}$  of over than 13.5 kV (Fig. 12 (b)). Meanwhile, in the reverse ESD event, the GaN ESD clamp conduct current in diode mode and has a low reverse triggering voltage. And the changes in L-FER's number nearly have no effect on the GaN ESD clamp's reverse triggering voltage.

## V. CONCLUSION

In this work, we carried out the experimental investigation and model analysis on a GaN ESD clamp, which features a discharge HEMT and a voltage divider formed by a L-FER chain and a resistor in series. The specific influence of the L-FER's number and resistor's value on the GaN ESD clamp's characteristic has been shown clearly. Both the clamp's static  $V_{\text{T,F}}$  and  $V_{\text{trig,F}}$  are increased with the increase in the L-FER's number and the decrease in the resistor's value. And we proposed an analytical model to analyze the dependence of the clamp's static  $V_{\text{T}}$  on the L-FER's number and resistor's value. The analytical model exhibits a good consistency with the experimentally measured results, which confirms the validity of the presented analytical model. The experimental investigation and model analysis of this work can be used to direct the design of the GaN ESD clamp, and save a lot of manpower, material resources and time costs.

## REFERENCES

- [1] A. Volke and M. Hornkamp, *IGBT Modules Technologies, Driver and Application*. Munich, Germany: Infineon Technol. AG, 2012, ch. 6.
- [2] K. Komatsu et al., "Study of unique ESD tolerance dependence on backgate ratio for RESURF LDMOS with rated voltage variation," in *Proc. 33rd Int. Symp. Power Semicond. Devices ICs (ISPSD)*, 2021, pp. 315–318, doi: [10.23919/ISPSD50666.2021.9452267](https://doi.org/10.23919/ISPSD50666.2021.9452267).
- [3] D.-W. Lai, G. de Raad, W. Tseng, T. Smedes, and A. J. Huijsing, "Bidirectional ESD protection device using PNP with pMOS-controlled Nwell bias," *IEEE Electron Device Lett.*, vol. 39, no. 3, pp. 331–334, Mar. 2018, doi: [10.1109/LED.2018.2795253](https://doi.org/10.1109/LED.2018.2795253).
- [4] D. Lai, G. de Raad, S. Sque, W. Peters, and T. Smedes, "High-voltage ESD protection device with fast transient reaction and high holding voltage," *IEEE Trans. Electron Devices*, vol. 66, no. 7, pp. 2884–2891, Jul. 2019, doi: [10.1109/TED.2019.2917264](https://doi.org/10.1109/TED.2019.2917264).
- [5] B. Shankar and M. Shrivastava, "Unique ESD behavior and failure modes of AlGaN/GaN HEMTs," in *Proc. IEEE Int. Rel. Phys. Symp. (IRPS)*, 2016, pp. 1–5, doi: [10.1109/IRPS.2016.7574608](https://doi.org/10.1109/IRPS.2016.7574608).
- [6] B. Shankar, S. Raghavan, and M. Shrivastava, "ESD reliability of AlGaN/GaN HEMT technology," *IEEE Trans. Electron Devices*, vol. 66, no. 9, pp. 3756–3763, Sep. 2019, doi: [10.1109/TED.2019.2926781](https://doi.org/10.1109/TED.2019.2926781).
- [7] J. Feng et al., "The ESD behavior of enhancement GaN HEMT power device with p-GaN gate structure," in *Proc. IEEE Int. Power Electron. Appl. Conf. Expo. (PEAC)*, 2018, pp. 1–4, doi: [10.1109/PEAC.2018.8590242](https://doi.org/10.1109/PEAC.2018.8590242).
- [8] E. Canato et al., "ESD-failure of E-mode GaN HEMTs: Role of device geometry and charge trapping," *Microelectron. Rel.*, vols. 100–101, pp. 1–8, Sep. 2019, doi: [10.1016/j.microrel.2019.06.026](https://doi.org/10.1016/j.microrel.2019.06.026).
- [9] Y. Q. Chen et al., "Degradation behavior and mechanisms of E-mode GaN HEMTs with p-GaN gate under reverse electrostatic discharge stress," *IEEE Trans. Electron Devices*, vol. 67, no. 2, pp. 566–570, Feb. 2020, doi: [10.1109/TED.2019.2959299](https://doi.org/10.1109/TED.2019.2959299).
- [10] X. B. Xu et al., "Analysis of trap and recovery characteristics based on low-frequency noise for E-mode GaN HEMTs under electrostatic discharge stress," *IEEE J. Electron Devices Soc.*, vol. 9, pp. 89–95, 2021, doi: [10.1109/JEDS.2020.3040445](https://doi.org/10.1109/JEDS.2020.3040445).
- [11] Y. Xin et al., "Electrostatic discharge (ESD) behavior of p-GaN HEMTs," in *Proc. 32nd Int. Symp. Power Semicond. Devices ICs (ISPSD)*, Vienna, Austria, Aug. 2020, pp. 317–320, doi: [10.1109/ISPSD46842.2020.9170063](https://doi.org/10.1109/ISPSD46842.2020.9170063).
- [12] K. J. Chen et al., "GaN-on-Si power technology: Devices and applications," *IEEE Trans. Electron Devices*, vol. 64, no. 3, pp. 779–795, Mar. 2017, doi: [10.1109/TED.2017.2657579](https://doi.org/10.1109/TED.2017.2657579).
- [13] W. Chen, K.-Y. Wong, and K. J. Chen, "Single-chip boost converter using monolithically integrated AlGaN/GaN lateral field-effect rectifier and normally off HEMT," *IEEE Electron Device Lett.*, vol. 30, no. 5, pp. 430–432, May 2009, doi: [10.1109/LED.2009.2015897](https://doi.org/10.1109/LED.2009.2015897).

- [14] X. Li et al., "Demonstration of GaN integrated half-bridge with on-chip drivers on 200-mm engineered substrates," *IEEE Electron Device Lett.*, vol. 40, no. 9, pp. 1499–1502, Sep. 2019, doi: [10.1109/LED.2019.2929417](https://doi.org/10.1109/LED.2019.2929417).
- [15] X. Li et al., "GaN-on-SOI: Monolithically integrated all-GaN ICs for power conversion," in *Proc. IEEE Int. Electron Devices Meeting (IEDM)*, 2019, pp. 1–4, doi: [10.1109/IEDM19573.2019.8993572](https://doi.org/10.1109/IEDM19573.2019.8993572).
- [16] Z. Wang, J. J. Liou, K.-L. Cho, and H.-C. Chiu, "Development of an electrostatic discharge protection solution in GaN technology," *IEEE Electron Device Lett.*, vol. 34, no. 12, pp. 1491–1493, Dec. 2013, doi: [10.1109/LED.2013.2283865](https://doi.org/10.1109/LED.2013.2283865).
- [17] C. Zhou et al., "On-chip gate ESD protection for AlGaN/GaN E-mode power HEMT delivering >2kV HBM ESD capability," in *Proc. IEEE 7th Workshop Wide Bandgap Power Devices Appl. (WiPDA)*, 2019, pp. 175–176, doi: [10.1109/WiPDA46397.2019.8998945](https://doi.org/10.1109/WiPDA46397.2019.8998945).
- [18] Z. He et al., "A novel AlGaN/GaN transient voltage suppression diode with bidirectional clamp capability," *Micromachines*, vol. 13, no. 22, p. 299, Feb. 2022, doi: [10.3390/mi13020299](https://doi.org/10.3390/mi13020299).
- [19] B. Yao et al., "A novel bidirectional AlGaN/GaN ESD protection diode," *Micromachines*, vol. 13, no. 22, p. 135, Jan. 2022, doi: [10.3390/mi13010135](https://doi.org/10.3390/mi13010135).
- [20] "p-GaN HEMT of EPC." [Online]. Available: <https://epc-co.com/epc/Products/eGaNFETsandICs.aspx>
- [21] S. Huang et al., "Current transport mechanism of Au/Ni/GaN Schottky diodes at high temperatures," *Appl. Phys. Lett.*, vol. 91, no. 7, Jul. 2007, Art. no. 72109, doi: [10.1063/1.2772182](https://doi.org/10.1063/1.2772182).
- [22] Y. Shi, X. Luo, H. Wang, W. Chen, and X. Yang, "Effects of etching temperature on the characteristics of recessed-anode AlGaN/GAN Schottky barrier diodes," *J. Electron. Mater.*, vol. 50, pp. 6291–6296, Aug. 2021, doi: [10.1007/s11664-021-09168-0](https://doi.org/10.1007/s11664-021-09168-0).